# Evidence for the First Phase of the Reprotonation Switch of Bacteriorhodopsin from Time-Resolved Photovoltage and Flash Photolysis Experiments on the Photoreversal of the M-Intermediate

Stefan Dickopf and Maarten P. Heyn
Biophysics Group, Department of Physics, Freie Universität Berlin, D-14195 Berlin, Germany

ABSTRACT  The kinetics of the photoreversal reaction of the M-intermediate of bacteriorhodopsin (bR) was investigated by time-resolved optical absorption spectroscopy and photovoltage measurements using double-flash excitation (a green flash (532 nm) followed by a blue flash (400 nm) after a variable delay). The sign of the photovoltage and the $^1H/^2H$ kinetic isotope effect indicate that the Schiff base is reprotonated by a group between the Schiff base and the extracellular surface, probably Asp[85]. Analysis of the kinetic data shows that the charge movement in 150 mM KCl at 12°C is characterized by two components with time constants of ~100 ns and ~600 ns, respectively, which are independent of the delay time between the flashes and the pH. The amplitudes of the fast and slow components depend on the delay and the pH. The slower component starts to contribute to the charge movement only after delays longer than 100 $\mu$s, is absent at low pH, and increases in amplitude with a $pK_a$ of ~6. Because the proton release group deprotonates after 70–100 $\mu$s and has a transient $pK_a$ of 5.8, these results suggest the following assignment: the fast and the combination of fast and slow components represent photoreversal from two M states, with the release group protonated and deprotonated, respectively. The slow phase of the photoreversal starts from a state with the release group deprotonated, and with the pK of Asp[85] elevated, and is probably due to the restoration of the pK of Asp[85] to its initial low value. This provides further evidence for coupling between the pK's of Asp[85] and the release group and suggests that proton release is the first step in the reprotonation switch. At alkaline pH the amplitude of the electrical signal from the back photoreaction decreases with an apparent pK of 8, without a corresponding decrease in the amount of M. At neutral pH the movement of the positively charged guanidinium group of Arg[82] from a position near the release group on the surface to Asp[85] makes a substantial contribution to the electrical photoreversal amplitude. Above the pK of the release group in the unphotolysed state (~8), Arg[82] stays near the surface, leading to a corresponding signal reduction.

## INTRODUCTION

Bacteriorhodopsin (bR) is a light-driven proton pump (Ebrey, 1993; Lanyi, 1993). The M-intermediate in the photocycle of bR plays a key role in the understanding of the mechanism of unidirectional proton transport. During the formation of M, a proton is transferred from the Schiff base to Asp[85], and concurrently a proton is released on the extracellular surface, presumably by Glu[204] (Brown et al., 1995). During the decay of M, the Schiff base is reprotonated from Asp[96], which in turn is reprotonated from the cytoplasmic side of the membrane. This change in connectivity of the Schiff base from Asp[85] to Asp[96], which occurs on opposite sides of the chromophore, during the lifetime of M, is referred to as the "reprotonation switch." Understanding its molecular mechanism is the subject of intense study by numerous investigators. A comprehensive discussion of the current understanding of the reprotonation switch has recently appeared (Richter et al., 1996). A distinction was made between "affinity" and "accessibility" mechanisms, in which the vectoriality of proton transport is achieved by

coordinated changes in the pK's or by structural changes, which block the access and change the connectivity of the groups involved, respectively. The reprotonation switch was decomposed into three phases (Richter et al., 1996). It was suggested that at neutral pH the first phase consists of proton release, i.e., the deprotonation of Glu[204]. Because of the linkage of the proton affinities of Asp[85] and Glu[204] (Balashov et al., 1993, 1995, 1996; Govindjee et al., 1996; Scharnagl and Fischer, 1996; Richter et al., 1996; Sampogna and Honig, 1996), the deprotonation of Glu[204] raises the pK of Asp[85], thereby shifting the proton equilibrium between the Schiff base and Asp[85] even further to the side of Asp[85] and preventing proton transfer back to the Schiff base (Richter et al., 1996; Balashov et al., 1996). This initial phase of the reprotonation switch would thus be of the "affinity" type. The two substates of M with the release group protonated and deprotonated were first introduced by Zimányi et al. (1992) and were called $M_1(XH)$ and $M_1'(X^-)$. (At the time the unknown release group was called XH.) In the second step of the reprotonation switch, the Schiff base is supposed to become accessible from Asp[96]. At neutral pH this is the $M_1'$-to-$M_2'$ transition, in the notation of Zimányi et al. (1992).

A blue light flash (400 nm) during the lifetime of M will lead to rapid isomerization of the chromophore to a state M' (all-*trans*; not to be confused with $M_1'$). In a following thermal transition the Schiff base is reprotonated, probably

---

Address reprint requests to Dr. Maarten P. Heyn, Biophysics Group, Department of Physics, Freie Universität Berlin, Arnimallee 14, D-14195 Berlin, Germany. Tel.: 49-30-838-6174; Fax: 49-30-838-5186; E-mail: heyn@physik.fu-berlin.de.

from Asp$^{85}$, and the system returns to bR in several hundred nanoseconds. A comprehensive review of the back photo-reactions of all of the photointermediates of bR has recently appeared (Balashov, 1995). It was shown by time-resolved optical absorption spectroscopy at room temperature that the return to bR proceeds via M', which absorbs at 380 nm, that the decay of M' occurs in ~200 ns, and that the reprotonation of the Schiff base occurs from an internal proton donor (Kalisky et al., 1978, 1981). Low-temperature steady-state Fourier transform infrared (FTIR) experiments suggest that this donor is Asp$^{85}$ (Takei et al., 1992). Double-flash experiments with a variable delay between the initial green flash and the second blue flash detected a single time constant for the M'-to-bR transition, which varied from 100 to 250 ns when the delay was increased from 10 to 200 $\mu$s (Druckmann et al., 1992). These data were interpreted as evidence of a transition between two sequential M states, which may correspond to $M_1'$ and $M_2'$ in the scheme of Zimányi et al. (1992).

Previous steady-state and time-resolved electrical measurements on the back photoreaction of M revealed that the charge movement is fast and that positive charge is moved in a direction opposite that observed for proton pumping (Karvaly and Dancsházy, 1977; Dancsházy et al., 1978; Hwang et al., 1978; Ormos et al., 1980). With a time resolution of 2 $\mu$s, a time constant of ~10 $\mu$s was obtained for the charge displacement at room temperature (Ormos et al., 1980). Thus, surprisingly, the charge movement associated with the M'-to-bR transition would be much slower than the time constant of 200 ns determined optically for the reprotonation of the Schiff base (Kalisky et al., 1978). With improved time resolution and data analysis, we show here that there is no discrepancy between the kinetics of optical and electrical signals for the back photoreaction of M.

In this study we investigated the kinetics of the back photoreaction of M, with the goal of obtaining evidence for the various phases of the reprotonation switch. By changing the delay between the flashes from 10 $\mu$s to 500 ms, it is possible to probe the back photoreaction from the various early and late substates of M. Because proton release occurs about 70–100 $\mu$s after the flash (Alexiev et al., 1995; Liu, 1990), it may be possible to distinguish between $M_1(XH)$ and $M_1'(X^-)$ on the basis of differences in the kinetics of the back photoreaction as a function of the delay. Such differences are expected, because the pK of Asp$^{85}$ is higher in $M_1'(X^-)$ than in $M_1(XH)$, as a consequence of the coupling between the pK's of Asp$^{85}$ and Glu$^{204}$ (Balashov et al., 1996; Richter et al., 1996). Moreover, because the transient pK of Glu$^{204}$ in M is ~5.8 (Zimányi et al., 1992), the state $M_1'(X^-)$ is not populated at low pH, and clear-cut pH effects are expected in the back photoreaction. From time-resolved photoelectrical and optical absorption measurements of the back photoreaction of M with pH and time delay as parameters, we have obtained further evidence that the initial step of the reprotonation switch is the proton release, as suggested by Richter et al. (1996).

Little is known about the mechanism of the linkage between Asp$^{85}$ and Glu$^{204}$, which are ~14 Å apart in the structure. It has been suggested that Arg$^{82}$ may assume alternative positions in the course of the cycle, being close to Asp$^{85}$ in the unphotolyzed state and moving to the vicinity of Glu$^{204}$ in M (Scharnagl and Fischer, 1996). This movement would provide a possible mechanism for the coupling between Asp$^{85}$ and Glu$^{204}$. Such a motion of the positively charged guanidinium group of Arg$^{82}$ is expected to make a substantial contribution to the amplitude of the electrical charge movement during the formation of M and in the back-reaction from M' to bR. The large decrease in the amplitude of the electrical back photoreaction at alkaline pH provides evidence for such a change in the position of Arg$^{82}$ in the course of the cycle.

## MATERIALS AND METHODS

The time-resolved photovoltage measurements were performed with the method of capacitative coupling, in which purple membranes are adsorbed to a lipid-impregnated support foil, as described (Holz et al., 1988; Moltke et al., 1995). The experimental setup for the electrical double-flash experiments is shown in Fig. 1. The first flash is from a frequency doubled Nd:YAG laser at 532 nm (10 ns, 10 mJ). The second flash is from an excimer laser pumped dye laser (15 ns, ~5 mJ, depending on the dye). The laser dyes used were Stilben3 (420 nm), PBBO (2-(4-Biphenylyl)-6-phenylbenzoxazol, 400 nm), and Rhodamin6G (580 nm). The delay between the two flashes can be varied from 1 $\mu$s to 100 ms (see legend to Fig. 1). To ensure homogeneous illumination of the foil with both flashes, it was necessary to reduce its diameter to 5 mm. This led to a reduction in the capacity of the foil, which was compensated by using a thinner foil of only 2 $\mu$m thickness. The resulting system discharge time of ~3 s is entirely adequate for these measurements. To resolve the fast signal of the M back photoreaction, the voltage amplifier was redesigned. Digitalization was performed by a fast storage scope, as described elsewhere (Dickopf et al., 1995). The Ag/AgCl electrodes were replaced by light-insensitive Pt elec-
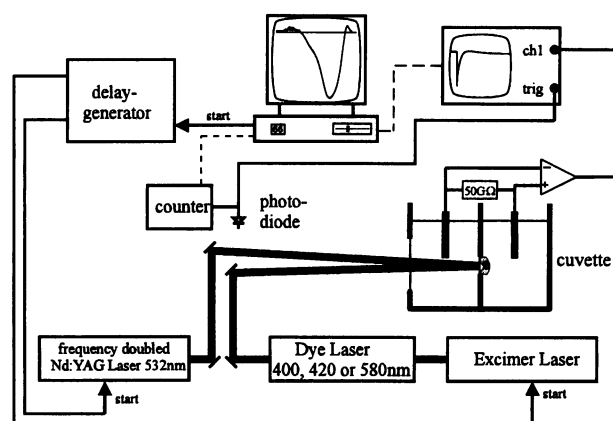


FIGURE 1 Experimental setup for the electrical double-flash experiments. Excitation is achieved by a nanosecond green flash (532 nm) followed by a nanosecond blue flash (400 or 420 nm) after a variable delay, as described in Materials and Methods. The cuvette consists of two compartments separated by a 2-$\mu$m piece of polyethylene foil. The delay between the flashes can be varied from 1 $\mu$s to several minutes (300-ns error) and is checked by a counter. With color filters in front of the photodiode, it is possible to trigger the acquisition system on the first or the second flash.

trodes. Together these improvements led to an apparent rise time of 30–40 ns for the formation of the positive voltage due to the K intermediate (see, e.g., Fig. 5 A), reflecting the instrumental rise time of the whole setup. All electrical measurements were performed in a 3 mM Tris HEPES Na-acetate buffer. Salt concentrations are as indicated. Titrations were carried out with NaOH and $H_2SO_4$.

Optical flash spectroscopy was performed with the apparatus described elsewhere (Otto et al., 1989), with the same laser systems and delay electronics as for the electrical measurements, but with the following modifications. The amplifier of the photomultiplier was replaced by one with higher bandwidth (80 MHz). To suppress more of the stray light from the flash, a double monochromator of small bandwidth was used ($\Delta\lambda$ = 5 nm). The 406-nm line of a mercury arc lamp was used as the probe beam, i.e., below the wavelength of the blue excitation flash (420 nm). This minimizes the error due to stray light from the flash and ensures a good signal-to-noise ratio, even for fast times. These modifications led to an instrumental rise time of 20–30 ns, as determined from the apparent formation of the K intermediate. Several series of measurements, with varying time delays between the flashes, were performed in 10% poly-acrylamide gels to immobilize the patches (Otto et al., 1995). The purpose of this was to fix the orientational distribution of the excited and unexcited transition dipole moments produced by the first flash. Otherwise, the rotational diffusion of the membranes would lead to time-dependent orientational distributions and a correction factor $f_1$ (see Results), which would depend on the delay. To obtain the maximum signal from the second flash (vertically polarized), the measuring light was also vertically polarized. The first flash excites the sample isotropically as described (Otto et al., 1995). This polarization geometry has the advantage of also allowing measurements in suspension (pH dependence at fixed delay), because an isotropic orientational distribution will remain isotropic when rotational diffusion occurs. The optical measurements were performed in a solution of 10 mM Tris buffer and salt, as indicated.

## RESULTS

### Optical double-flash experiments

Typical transient absorption data for the back photoreaction of M at 406 nm are shown in Fig. 2, A and B. The photo-reversal of M is evident from trace 2 of Fig. 2 A, where the blue flash excitation occurs 500 $\mu$s after the initial green flash excitation. The back photoreaction is clearly fast compared to the L-to-M transition, and cannot be resolved by using a logarithmic time base when triggering on the first flash. The rise of the back photoreaction (trace 2) can be resolved, however, by triggering on the second flash (Fig. 2 B). At the time of the second flash there exists, in general, a mixture of all intermediates K, L, M, N, and O, as well as the remaining population of bR molecules that where not excited by the first flash. The mixture depends on the time delay between the flashes. The blue flash is able to excite all of these intermediates. Therefore, contributions from the back photoreaction of all intermediates may occur, in principle. To estimate the magnitude of contributions from photoreactions of intermediates other than M, control experiments were performed with a second flash at 580 nm, which excites bR as well as all intermediates except M. These control experiments reveal that for transient absorption measurements at 406 nm, there is no contribution from intermediates other than M on the time scale of the M back photoreaction (data not shown). Therefore, we need only correct for the fraction of bR molecules that are not excited
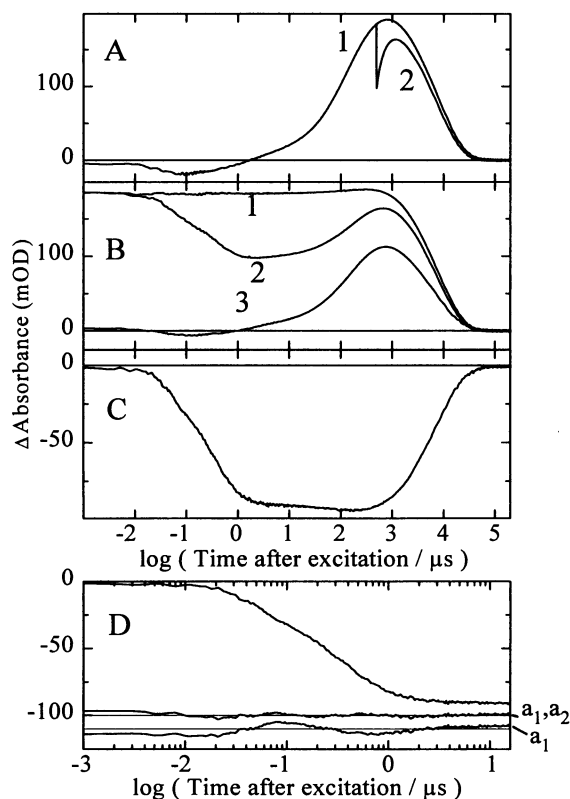


FIGURE 2   Optical absorbance changes at 406 nm after single- (532 nm) or double- (532/420 nm) flash excitation. Note the logarithmic time scale. (A) Kinetics of the rise and decay of the M-intermediate with excitation by the 532-nm flash (trace 1), and with a second blue flash (420 nm) arriving 500 $\mu$s after the green flash (trace 2). (B) The same traces (1 and 2), but with the logarithmic data acquisition triggered on the second flash. This allows one to resolve the fast photoreversal of M, which was not resolved in A. Trace 3 is the signal due to M when the blue flash alone excites the sample. (C) Signal for the back photoreaction of M after correction for the excitation of the remaining ground-state bR molecules by the second blue flash obtained from traces 1, 2, and 3 of B according to Eq. 1, with $f_1$ = 0.6 (see text). (D) The rise time part of C, shown on an expanded time scale (upper trace). The lower two traces are the residuals for a fit with one (315 ns, $a_1$) or two (70 ns, 32%, $a_1$; 480 ns, 68%, $a_2$) exponentials. Conditions: 150 mM KCl, pH 7.0, 15°C.

by the first green flash but may be excited by the second blue flash. At saturation, the first flash drives at most 40% of the bR molecules in the photocycle. The remaining 60% may thus be excited by the second blue flash. Trace 3 of Fig. 2 B shows that indeed the blue flash alone is quite efficient in inducing the photocycle. Thus the signal due to the M back photoreaction $\Delta A_M(t)$ may be obtained from traces 1, 2, and 3 in the following way:

$$\Delta A_M(t) = \Delta A_2(t) - \Delta A_1(t) - f_1 \Delta A_3(t) \qquad (1)$$

where $\Delta A_2(t)$ is the time trace for the double-flash experiment (trace 2 of Fig. 2 B), $\Delta A_1(t)$ is the time trace of the first flash alone (trace 1 of Fig. 2 B), $\Delta A_3(t)$ is the time trace for the second flash alone (trace 3 of Fig. 2 B), and $f_1$ is the fraction of the initial bR population not excited by the first flash. A small error is made in the substraction according to

Eq. 1, because $\Delta A_3(t)$ does not correct for the saturation effect that occurs when the first flash leads to strong excitation. These cooperativity effects (e.g., Dancsházy and Tokaji, 1993) arise in the second half of the photocycle in the time domain beyond 1 ms and are irrelevant for the back photoreaction that occurs on the submicrosecond time scale.

One way to determine $f_1$ is by measuring the amplitude of the ground-state depletion signal at 570 nm. Doing this, one finds that $f_1 \approx 0.7$. Because of the spectral overlap with other intermediates at this wavelength (K, L, N, O), however, this estimate is too large. A more accurate way to determine $f_1$ is to perform double-flash experiments at 532/ 580 nm, with the monitoring wavelength set at 635 nm. This allows the extra amount of K produced by the second flash to be determined accurately and leads to a constant value of $f_1 = 0.6$ over the range of delay times where M exists. For larger delay times $f_1$ increases to 1 because of the recovery of bR. Fig. 2 C shows how the back photoreaction signal of M is obtained from traces 1, 2, and 3 of Fig. 2 B with $f_1 = 0.6$. We note that the results for the kinetics of the M back photoreaction are rather insensitive to the precise value of $f_1$, because of the very small amplitude of trace 3 of Fig. 2 B for times shorter than 2 $\mu$s. Fig. 2 C shows that under the given experimental conditions, when the delay time is 500 $\mu$s, the back photoreaction signal has a fast rise time of a few hundred nanoseconds and remains approximately constant during the time interval between 1 $\mu$s and 1 ms. The negative M population then decays as expected in a few milliseconds, corresponding to the decay of the M intermediate. In Fig. 2 D, the increase in the M photoreversal signal is shown on an expanded time scale. A fit with a single exponential (315 ns, $a_1$) shows systematic deviations in the residuals (trace labeled $a_1$ in Fig. 2 D). Therefore, two exponentials are clearly required for a proper fit. The residuals for the fit with two exponentials is satisfactory (trace labeled $a_1$, $a_2$ in Fig. 2 D). The relative amplitudes are 32% ($a_1$, 70 ns) and 68% ($a_2$, 480 ns).

Similar experiments were performed in which the time delay between the two flashes was varied from 20 $\mu$s to 20 ms, i.e., essentially over the whole time range where M exists. Fig. 3 A shows that for each delay, two rise times, $\tau_1$ and $\tau_2$, are required and that they are independent of the value of the time delay to a good approximation. A global fit of the data at all delay times with the same two exponential time constants of 120 and 630 ns is thus justified. Fig. 3 B shows the amplitudes $a_1$ and $a_2$, corresponding to the two rise times $\tau_1$ and $\tau_2$, as a function of the delay (global fit). At each delay time, both components are required, but their relative contributions depend on the delay time. For short delays, the fast component $a_1$ dominates, whereas for longer delays the $a_2$ component is larger. The cross-over point is $\sim$200 $\mu$s. The sum of $a_1$ and $a_2$ is roughly proportional to the absorption change $\Delta A(t)$ at 406 nm (see Fig. 3 B). This is expected because $\Delta A(t)$ reflects the M population generated by the first flash.
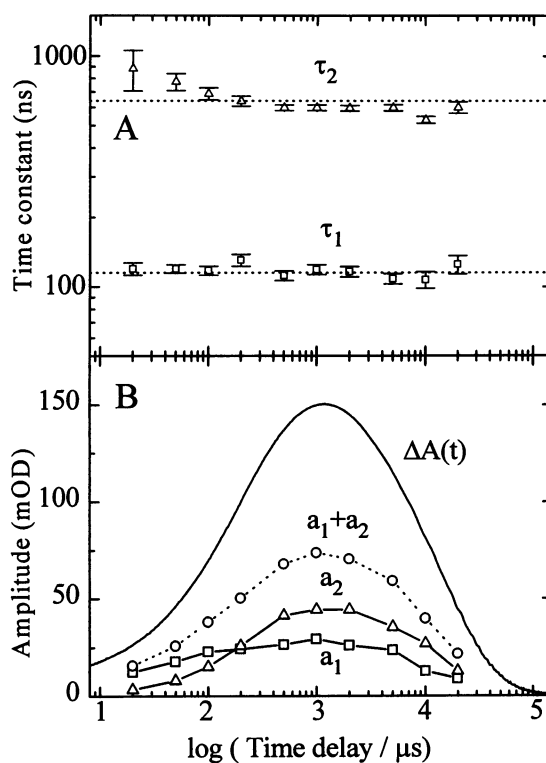


FIGURE 3  (A) Dependence of the rise times $\tau_1$ and $\tau_2$ of the photoreversal absorbance signal at 406 nm on the time delay. (B) Dependence of the corresponding amplitudes $a_1$ and $a_2$ on the time delay in a global fit with $\tau_1 = 120$ ns and $\tau_2 = 630$ ns. $\Delta A(t)$ is the absorbance change at 406 nm and reflects the formation and decay of the M population generated by the first flash. Conditions: 150 mM KCl, pH 7.5, 12°C, $f_1 = 0.65$, 10% polyacrylamide gel.

## Electrical double-flash experiments

As for the optical measurements, we first discuss the control experiments in which two green flashes (532/580 nm) are used. These experiments are designed to test if the second flash leads to back photoreaction signals from intermediates other than M (which does not absorb at 580 nm). When the second flash has a wavelength of 420 or 400 nm, as in the photoreversal of M, contributions from other intermediates may still occur, because they all absorb at these higher energies, albeit with lower probability than at 580 nm. Trace 1 in Fig. 4 A shows the normal time-resolved photovoltage signal after single-flash excitation at 532 nm. The return to the baseline, starting at $\sim$100 ms, is due to the passive system discharge. Trace 2 in Fig. 4 A shows that when a second 580-nm flash is fired after a delay of 50 $\mu$s, additional charge motion occurs in the forward direction. In Fig. 4 B the same data are shown, but now with the acquisition system triggered on the second flash (traces 1 and 2). Also shown (trace 3) is the signal due to the second flash alone. If the second flash (580 nm) does not generate any electrogenic charge motion from back photoreactions of the K, L, N, and O intermediates, the difference between 1 and 2 must be due entirely to the excitation by the second flash of the
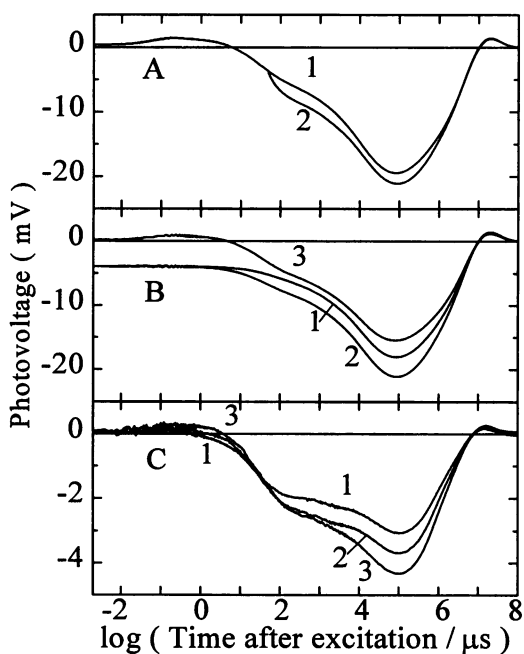
FIGURE 4   Electrical double-flash experiment with two green flashes (532/580 nm). (A) Trace 1: Photovoltage signal after single flash excitation at 532 nm. The return of the signal to zero, starting around 100 ms, is due to the system's discharge through the high impedance resistor. Trace 2: The second 580-nm flash arrives 50 $\mu$s after the first 532-nm flash, giving rise to an additional voltage. (B) Traces 1 and 2 of A are shown again, but with the data acquisition triggered on the second flash. Trace 3 is the photovoltage induced by the second flash alone. (C) The difference between traces 1 and 2 of B at a delay of 50 $\mu$s (trace 1). Traces 2 and 3 are the corresponding differences with delay times of 500 $\mu$s and 5 ms, respectively. Conditions for all panels: 150 mM $K_2SO_4$, pH 6.0, 22°C.

remaining 60–70% of the bR population that was not excited by the first flash. In this case, the difference 2–1 should be proportional to 1 of Fig. 4 A or 3 of Fig. 4 B. In Fig. 4 C these differences are plotted for delays of 50 $\mu$s (trace 1), 500 $\mu$s (trace 2), and 5 ms (trace 3). Comparing these with trace 1 of Fig. 4 A, it is apparent that their shapes are different. There are two major differences. The first is that the ratio of the amplitudes of the charge motion between 10–100 $\mu$s (L to M) and 5–50 ms (M decay) is much larger in Fig. 4 C than in trace 1 of Fig. 4 A. This is not due to backreactions from L or N, because, at a delay of 500 $\mu$s, only the states M and bR are populated with very minor contributions from L and N (trace 2 of Fig. 4 C). This effect is most likely due to the interaction with the electric field built up across the membrane by the first saturating flash, which slows the millisecond charge motion induced by the second flash to such an extent that it becomes as slow or slower than the system discharge time. As a consequence, the amplitude of this millisecond component is reduced, as observed. The second difference is that the difference signal at early times (50 ns to 10 $\mu$s) depends on the delay (Fig. 4 C, traces 1, 2, and 3). The first positive phase of the normal photovoltage signal in this time range (see Fig. 4 A, trace 1) is absent in Fig. 4 C, trace 1 (the time delay is 50 $\mu$s, when

the L state is populated), but regains amplitude with increasing delays, when less or no L remains (Fig. 4 C, trace 2, 500 $\mu$s; Fig. 4 C, trace 3, 5 ms). This indicates that a fast electrical back photoreaction occurs from L. This charge motion is of polarity opposite that resulting from the M back photoreaction (see below). Fast components in the M back photoreaction will thus be reduced, because the back photoreaction signal from L overlaps that of M. Unfortunately, it is not possible to choose measuring conditions in which contributions from the L back photoreaction are completely absent, as in optical double-flash experiments. In principle, it is necessary to correct every 532/400-nm experiment with a 532/580-nm experiment, which is not practical. There are, however, two reasons why the electrical contribution from L may be neglected as a first approximation. The first is that the amplitude of the back photoreaction of L must be considerably smaller than that of M, as can be seen from the forward photovoltages developed in the L and M states (trace 1 of Fig. 4 A, for example). The second is that the effect described will be reduced in the 580/400-nm double-flash experiments, because of the smaller extinction coefficient of L at 400 nm compared to those at 580 nm. We therefore analyzed the electrical double-flash experiments with the second flash at 400 nm in the same way as the optical measurements, i.e.,

$$V_M(t) = V_2(t) - V_1(t) - f_1 V_3(t) \qquad (2)$$

which is the same as Eq. 1 for optical measurements, except that $\Delta A$ is replaced by the photovoltage $V$. This procedure is illustrated for the photoreversal of M at a delay time of 500 $\mu$s in Fig. 5. Fig. 5 A illustrates that the second 400-nm flash (trace 2) induces a fast photovoltage of polarity opposite that induced by a single flash (trace 1), which is not resolved when triggering on the first flash. Fig. 5 B shows the same events, but this time triggered on the second flash, and suggests that the rise time of trace 2 is several hundred nanoseconds. Also shown in Fig. 5 B, trace 3, is the photovoltage induced by the second 400-nm flash alone. Fig. 5 C shows the photoreversal voltage from M, calculated from traces 1, 2, and 3 of Fig. 5 B, using Eq. 2, with $f_1 = 0.65$, to correct for the ground-state excitation of bR. Fig. 5 D offers an expanded view of the formation of the photovoltage (upper trace), together with the residuals from fits with one ($u_1$) or two exponentials ($u_1$, $u_2$). The fit with the two exponentials ($\tau_1$: 130 ns ($u_1$ 58%); $\tau_2$: 780 ns ($u_2$ 42%)) is clearly superior. The faster component may not be completely resolved, because the instrumental rise time is ~30–40 ns, which is comparable to the observed 130 ns. The 100-ms component in the photovoltage in Fig. 5 C is an artefact. As explained above, the millisecond electrical component induced by the blue second flash is slowed down and reduced in amplitude by the membrane potential generated by the saturating green flash. The correction term $V_3$ in Eq. 2 does not take this effect of the membrane potential into account. This leads to the artifactual rise of the signal around 100 ms.
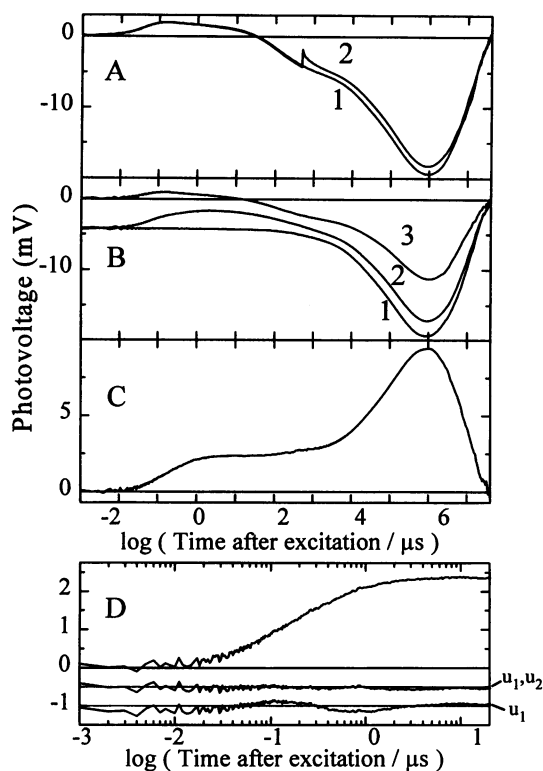
FIGURE 5   Photovoltage changes due to the back photoreaction of M. (A) Kinetics of the photovoltage after a 532-nm flash (*trace 1*) and when the 532-nm flash is followed by a 400-nm flash after a delay of 500 $\mu$s (*trace 2*). (B) Traces 1 and 2 of A, but with the data acquisition triggered on the second flash. Trace 3: Photovoltage due to the 400 nm flash alone. (C) Photovoltage due to the photoreversal of M obtained from traces 1, 2, and 3 of B, using Eq. 2, with $f_1$ = 0.65. (D) Expanded view of the formation of the photovoltage in C (*upper trace*). The lower two traces are the residuals from a fit with one (290 ns, $u_1$) or two (130 ns, 58%, $u_1$; 780 ns, 42%, $u_2$) exponentials. Conditions: 150 mM KCl, pH 7.0, 0.3°C.

These experiments were repeated with time delays varying between 10 $\mu$s and 500 ms. As in the optical measurements, two exponentials were required for each time delay, and the corresponding time constants were independent of the delay, justifying a global fit. Fig. 6 shows the amplitudes of the fast ($u_1$) and slow ($u_2$) components as a function of the delay at 150 mM KCl, pH 7.0, 0.3°C. As in the optical experiments, $u_1$ dominates for early times. The $u_2$ amplitude starts to increase after a delay of ~70 $\mu$s. The sum $u_1 + u_2$ rises parallel to the rise of M (Fig. 3 B), as expected. The decay of $u_1 + u_2$ is clearly an order of magnitude slower than the decay of M (Fig. 3 B). This is another manifestation of the feedback by the electrical field, which is built up by the first flash in the L→M transition, on the rate of the charge motion associated with the M decay.

## pH dependence

The optical and electrical double-flash experiments were performed over a broad range of pH values. These measurements were carried out at a fixed time delay of 500 $\mu$s,
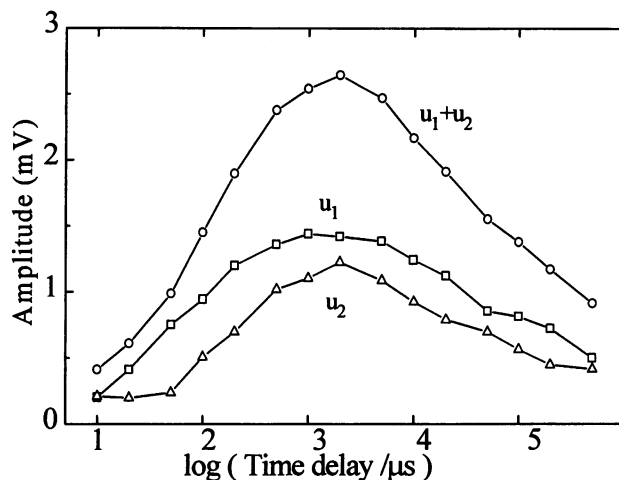


FIGURE 6   Dependence of the two electrical amplitudes, $u_1$ and $u_2$, of the M back photoreaction on the time delay between the green and blue flashes. Global fit with $\tau_1$ = 120 ns and $\tau_2$ = 700 ns. Conditions: 150 mM KCl, pH 7.0, 0.3°C, $f_1$ = 0.65.

where the M population is largest. The time constants were pH independent (allowing a global fit), whereas the amplitudes, shown in Fig. 7, are strongly pH dependent. The optical data (Fig. 7 A) imply a transition from a low-pH
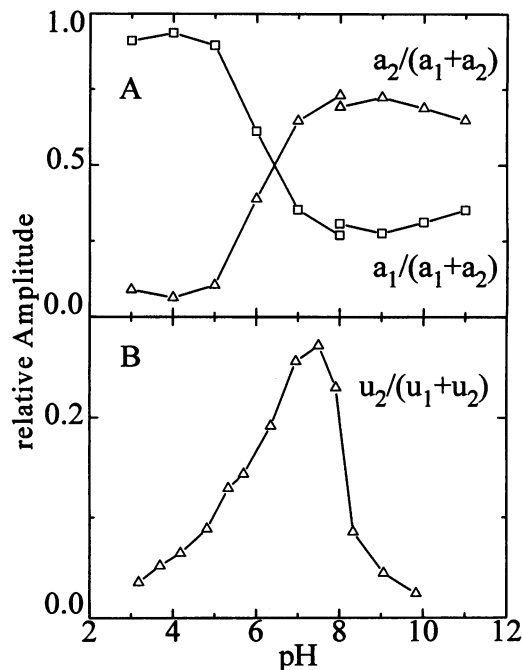


FIGURE 7   (A) pH dependence of the relative amplitudes of the two components, $a_1$ and $a_2$, of the M back photoreaction as measured optically. For this series of measurements we obtained $\tau_1$ = 90 ns and $\tau_2$ = 510 ns in the global fitting procedure. At pH 8 there are two data points, because two samples were used, for titration from pH 8 downward and upward, respectively. (B) pH dependence of the relative amplitude of the slower component $u_2$ of the electrical signal. Global fit with $\tau_1$ = 120 ns and $\tau_2$ = 700 ns. The titration was performed from high to low pH. Conditions: 150 mM KCl, 12°C, $f_1$ = 0.70, $\Delta t$ = 500 $\mu$s.

regime with $a_1$ dominating, to a high-pH regime with a 2:1 ratio of $a_2$ to $a_1$. The apparent pK is ~6. For the electrical data (Fig. 7 *B*) the relative contribution of $u_2$ also increases with pH, with an apparent pK of ~6. However, the contribution of $u_2$ never exceeds 40% and drops again to zero at higher pH with an apparent pK of 8.

It is of interest to compare these results with the pH dependence of the forward charge motion associated with the L-to-M transition. Fig. 8 shows that the amplitude of the forward microsecond electrical signal ($u_M$) decreases strongly in the alkaline region with a pK of ~8, whereas the amount of M ($a_M$) stays almost constant. An analogous drop is observed at alkaline pH in the total electrical photoreversal signal from M ($u_1 + u_2$).

## Kinetic isotope effects

The $^1H/^2H$ isotope effects on the kinetics of the back photoreaction of M are compared in Fig. 9 *B*, with the corresponding effects on the kinetics of the formation of M (Fig. 9 *A*). It is clear from these optical data that the isotope effects are much larger in the rise of M than in the photoreversal of M. Because the kinetics are multiexponential, a Gaussian distribution of exponentials was used for this comparison. This allows the kinetics to be characterized by a single time constant corresponding to the maximum of the distribution. In this way we find that $\tau_D/\tau_H = 6.8$ for the formation of M and $\tau_D/\tau_H = 1.7$ for the back photoreaction of M.

## Temperature dependence

The temperature dependence of the M back photoreaction was measured optically (from 10°C to 40°C at pH 8.0) and



FIGURE 9    (*A*) $^1H/^2H$ isotope effects in the rise and decay kinetics of the M intermediate as monitored at 406 nm. (*B*) $^1H/^2H$ isotope effects in the kinetics of the photoreversal of M as monitored optically at 406 nm. The time traces were obtained from double-flash experiments, using Eq. 1, with $f_1 = 0.57$ and $f_1 = 0.55$ for $^1H_2O$ and $^2H_2O$, respectively. The time delays were 1 ms ($^1H_2O$) and 2 ms ($^2H_2O$). Conditions: pH/pD 7, 150 mM KCl, 10°C.
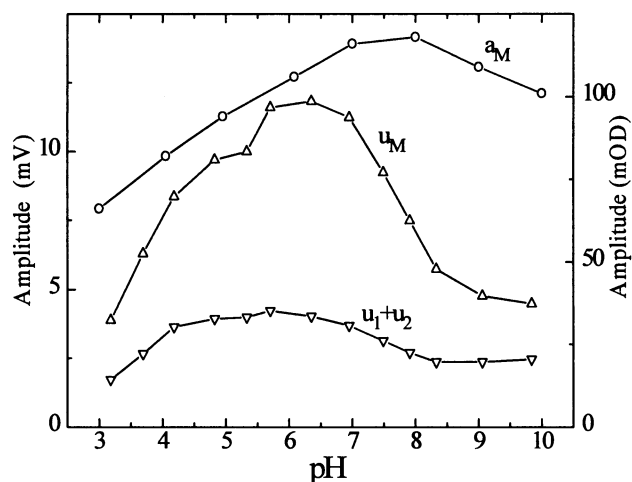


FIGURE 8    pH dependence of the optical and electrical amplitudes associated with the M intermediate. $a_M$ (○), Amount of the M intermediate as measured by the absorbance at 406 nm (*scale on the right*). $u_M$ (△), Amplitude of the electrical signal associated with the L to M transition (*scale on the left*). $u_1 + u_2$ (▽): Sum of the two electrical signals associated with the M' to bR back photoreaction (*scale on the left*). Conditions as in Fig. 7.
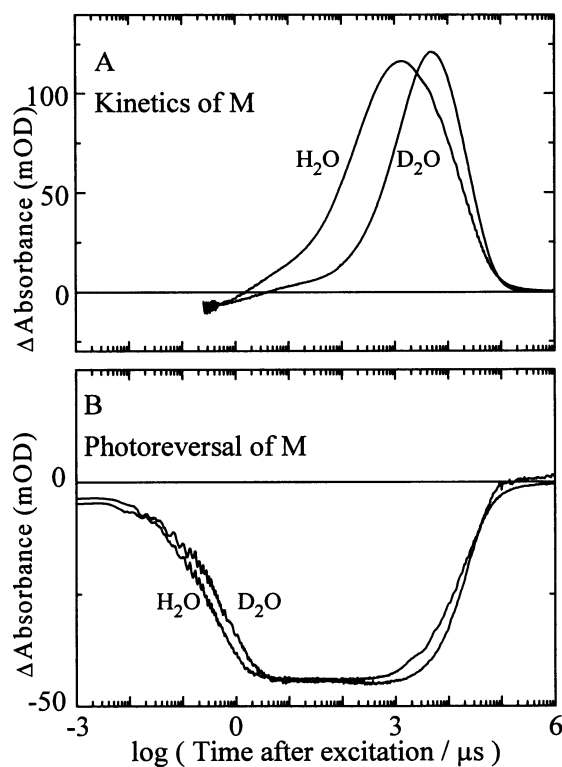
electrically (from 0.2°C to 37°C at pH 7.1) at 150 mM KCl, with a delay time of 500 $\mu$s. For convenience the signal was characterized by a Gaussian distribution of exponentials (Holz et al., 1988). The time corresponding to the maximum was plotted logarithmically versus $1/T$. In this way, activation energies of 37 and 27 kJ/mol were obtained for the optical and electrical signals, respectively (data not shown). For the L-to-M transition, we obtained activation energies of 61 and 60 kJ/mol from the optical and electrical signals, respectively (data not shown). The lower end of the temperature range was limited for the electrical measurements by the freezing of the suspension (0°C) and for the optical measurements by the condensation of water on the cuvette surface (10°C). In general, measurements were performed at low temperatures because of the improved time resolution.

## DISCUSSION

The initial step in the back photoreaction of M is the 13-*cis* → all-*trans* isomerization of the chromophore (Stockburger et al., 1979; Grieger and Atkinson, 1985). This rapid transition from M to M' is not resolved in our experiments. It is followed by the reprotonation of the Schiff base from Asp[85] (Takei et al., 1992). The $^1H/^2H$ kinetic isotope effect,

which we observed in the kinetics of the absorbance change at 406 nm (Fig. 9 $B$), is evidence that these signals are associated with proton transfer.

Our kinetic absorption data clearly show that the reprotonation of the Schiff base in the decay of M' occurs with two components for every delay (Figs. 2 and 3 $A$). At pH 7.5 (150 mM KCl), the time constants $\tau_1$ and $\tau_2$ are independent of the delay. The corresponding amplitudes $a_1$ and $a_2$ do depend on the delay (Fig. 3 $B$). At each delay the sum $a_1 + a_2$ is approximately proportional to the absorption change $\Delta A$ at 406 nm, which is the amount of M produced by the first green flash (Fig. 3 $B$). This is to be expected, because the amplitude of the back-reaction should be proportional to the population of the M state at that delay. For early delays the faster component $a_1$ dominates, whereas the slower component $a_2$ becomes largest at delays longer than 200 $\mu$s. This is close to the time of 70–85 $\mu$s, at which the proton is released at neutral pH (Alexiev et al., 1995; Liu, 1990). It was recently shown that a strong coupling exists between the pK's of the proton acceptor Asp[85] and the proton release group Glu[204] (Balashov et al., 1993, 1995, 1996; Govindjee et al., 1996; Richter et al., 1996). These studies provide evidence that proton release by Glu[204] leads to an increase in the pK and proton affinity of Asp[85]. This increase in the pK of Asp[85] after proton release ($\sim$100 $\mu$s) is expected to lead to a slower phase in the back photoreaction M' $\rightarrow$ bR, because the pK of Asp[85] has to be restored to its lower ground-state value. It is thus sensible to make the following assignments: $a_1$ is the fast reprotonation from Asp[85] with Glu[204] still protonated, and the combination of $a_1$ and $a_2$ is the slower reprotonation after proton release by Glu[204]. This assignment is supported by the fact that the amplitude of $a_2$ starts to grow after a lag phase of $\sim$200 $\mu$s. The pK of the release group was shown to drop from $\sim$9 in the unphotolyzed state to 5.8 in M (Zimányi et al., 1992). Thus for pH values much below 6, Glu[204] does not deprotonate during the cycle. Accordingly, only the faster component $a_1$ is expected to be observed. For pH values much above 6, Glu[204] is the proton release group, and mainly the slower component $a_2$ should be observed. The data of Fig. 7, at a delay of 500 $\mu$s, show that these predictions are indeed borne out.

Recently the reprotonation switch was reported to consist of three sequential phases (Richter et al., 1996). Proton release by Glu[204] was suggested to be the first phase, because it raises the pK of Asp[85], thereby shifting the fast proton equilibrium between the Schiff base and Asp[85] completely to the side of Asp[85]. Likewise in the back-reaction, the fast component probably represents the initial proton equilibrium between the Schiff base and Asp[85]. This equilibrium will shift to complete protonation of the Schiff base when the pK of Asp[85] returns to its initial low value. The transition between the high and low pK states of Asp[85] is the slow phase, which is followed by the rapid and complete transfer of the proton to the Schiff base. Movement of Arg[82] toward Asp[85] may be one way to restore the low pK of Asp[85]. This model clearly explains why the two components

coexist at long delays, whereas only the fast phase occurs at short delays. For delays shorter than the proton release time, the pK of Asp[85] did not increase, and only the fast component is observed.

The pK of $\sim$6, which we determined here from kinetic data at 12°C (Fig. 7), is in excellent agreement with steady-state measurements on the thermal stability of M' at low temperatures (Friedman et al., 1994). These authors reported that at $-150$°C, $\sim$72% of M' is converted to bR at pH 5, whereas this percentage dropped to 40% above pH 8. Titration showed that this transition occurs at a pK of $\sim$6 at 100 mM NaCl. These authors suggest that this is probably the pK of the proton release group at room temperature, and that this group apparently controls the thermal stability of M'. The thermal stability of M' against decay to bR increases at pH greater than 6, where Glu[204] can deprotonate during the cycle. We report here that the relative contribution of the slower decay component of M' increases with a pK of $\sim$6 (Fig. 7).

The slowing down of the photoreversal kinetics of M with increasing delay, as monitored by absorption spectroscopy, has previously been reported (Druckmann et al., 1992). These authors observed only a single time constant, however, which increased from 100 to 250 ns as the delay was increased from 10 to 250 $\mu$s (pH 7, 100 mM NaCl, room temperature). With our better time resolution and higher signal-to-noise ratio, it is now clear that two components are required, that the corresponding time constants do not depend on the delay, but that the relative contribution of the slower component increases with the delay.

The results of the electrical double-flash experiments support the interpretation of the transient absorption measurements. The sign of the voltage signal for the back photoreaction of M (Fig. 5) shows that the charge displacement product is opposite that of the proton pump process, indicating that the Schiff base is reprotonated from a group located between the Schiff base and the extracellular surface. This is in excellent agreement with the steady-state FTIR investigations, which showed that Asp[85] is the proton donor for this back-reaction (Takei et al., 1992). Two components, $u_1$ and $u_2$, with time constants of 120 and 700 ns (pH 7.0, 150 mM KCl, 0.3°C), were observed, which are most likely directly related to the fast and slow components, $a_1$ and $a_2$, in the absorption kinetics. In agreement with the optical data, the slow $u_2$ component starts to rise only after delays longer than 100 $\mu$s (Fig. 6) and increases in relative amplitude with an apparent pK of $\sim$6 (Fig. 7 $B$). These results thus strongly support the interpretation of the absorption data given above, that the combination of fast and slower components is associated with the reprotonation of the Schiff base in a state where Glu[204] is deprotonated (the first phase of the reprotonation switch).

Earlier time-resolved electrical studies of the back photoreaction of M were severely hampered by insufficient time resolution and by inadequate treatment of the corrections for excitation of unphotolyzed bR by the second flash (Dancsházy et al., 1978; Hwang et al., 1978; Ormos et al.,

1980). Despite these problems, it was established that the charge movement had polarity opposite that induced by the proton pump and that it was very fast. Dancsházy et al. (1978) reported that the rise time was faster than 5 $\mu$s at room temperature, whereas Ormos et al. (1980), using a blue flash of 2 $\mu$s pulse width, observed one component with a time constant of 10 $\mu$s at room temperature. The fast components reported here, which are clearly associated with the corresponding components in the absorbance signal, could not be resolved in these studies.

From a comparison of Fig. 9, A and B, it is clear that the kinetic isotope effect in the photoreversal of M is much smaller (1.7) than in the formation of M (6.8). This suggests that the mechanism of shifting the proton equilibrium from the Schiff base to $Asp^{85}$ in the formation of M differs from that in the reverse pathway from M$'$ to bR. Based on a recent analysis of $^1H/^2H$ isotope effects in the photocycle (le Coutre and Gerwert, 1996), this difference may be interpreted as follows. In the formation of M the equilibrium between the Schiff base and $Asp^{85}$ is shifted toward $Asp^{85}$, where this pK shift is coupled to another proton transfer in an icelike hydrogen-bonded network (probably via $Arg^{82}$), whereas in the reverse step it is coupled to a proton transfer that is similar to that in liquid water. During the lifetime of M there is apparently a change in structure in the extracellular channel. This change may well be part of the reprotonation switch, because this structural change slows down the kinetics of the proton return path. This step thus appears to be of the "accessibility" type. A structural change from an ice- to a waterlike structure should be accompanied by a change in polarizability. Such a change in polarizability in the whole proton release channel was already observed on the basis of FTIR difference spectra of the L and M intermediates (Olejnik et al., 1992). This change could be part of the second phase of the reprotonation switch, the $M_1'$-$M_2'$ transition, in the model of Richter et al. (1996). Further support for a difference in mechanism comes from the activation energies. For the M$'$ to bR reaction, values of 37 and 27 kJ/mol were obtained from the optical and electrical signals, respectively. This is only about half the value of 61 kJ/mol for the M formation.

There are three differences between the optical and electrical results that need further discussion:

1. The amplitude of the slow electrical component $u_2$ never exceeds 40% of the total amplitude, whereas the slow absorption amplitude $a_2$ is largest in all cases, except for delays shorter than 200 $\mu$s. The interpretation of the electrical amplitudes is more complicated than that of the optical data, because the voltage associated with a transition is proportional to the distance the charge moved as well as inversely proportional to the local instantaneous dielectric constant (Trissl, 1990; Moltke et al., 1995). The electrical amplitudes are therefore not related to the optical ones in a simple way. Moreover, the chromophore absorbance change at 406 nm monitors the local reprotonation of the Schiff base, whereas the electrical signal represents the charge motion throughout the whole protein. A good example of

this nonparallel behavior of the optical and electrical amplitudes is the alkaline transition with intrinsic pK of $\sim$8.2 (Kono et al., 1993; Liu, 1990). Above this pK the amplitude of the electrical signal in the microsecond time range associated with the L-to-M transition ($u_M$) drops to $\sim$35%, whereas the population of M ($a_M$) changes by only 20% (see Fig. 8). Thus, although the Schiff base still deprotonates upon excitation at pH 10, the distance over which charge is moved seems to be much reduced. It was suggested that the proton release step was abolished under these conditions (Liu, 1990; Kono et al., 1993).

2. Both $u_2$ and $a_2$ increase with an apparent pK of 6, but at alkaline pH, $u_2$ decreases again with an apparent pK of 8, whereas $a_2$ does not. We believe that this difference in pH dependence is due to the alkaline transition of bR described in 1. Our interpretation of this effect is as follows. The large electrical amplitude in the 10–100-$\mu$s time range (Fig. 4 A) cannot be due to the proton transfer from the Schiff base to $Asp^{85}$ alone. Although the dielectric constant in the neighborhood of $Asp^{85}$ may be quite low ($\sim$2 in M; Braiman et al., 1996), the distance is too short. Proton release from $Glu^{204}$ in an environment where the dielectric constant is large does not provide a satisfactory explanation either. A substantial contribution may come from the positively charged guanidinium group of $Arg^{82}$, however. If this group moves from a position close to $Asp^{85}$ to a position near $Glu^{204}$ on the extracellular surface (as proposed by Scharnagl and Fischer, 1996) when $Asp^{85}$ is protonated, the observed electrical amplitude has about the right magnitude (taking the more hydrophilic environment of $Arg^{82}$ in the proton release channel into account). With these two charge motions occurring in a concerted way, only one kinetic constant should be observed in the microsecond electrical signal. The movement of $Arg^{82}$ could also provide part of the coupling between $Asp^{85}$ and $Glu^{204}$. At alkaline pH, $Glu^{204}$ is already deprotonated in the unphotolyzed state. It has been suggested that above the pK of $Glu^{204}$, Arg is in the position near the extracellular side in the unphotolyzed state (Balashov et al., 1993; Scharnagl and Fischer, 1996) and remains associated with the negative charge of $Glu^{204}$ throughout the photocycle. The drop in the electrical amplitude $u_M$ at alkaline pH (Fig. 8) provides strong experimental support for this suggestion, because the contribution from the charge movement of $Arg^{82}$ is predicted to be absent. What remains is the charge motion from the Schiff base to $Asp^{85}$. This plausible interpretation for the pH dependence of the forward charge motion in the L-to-M transition has corresponding consequences for the reverse motion in the M$'$-to-bR transition. In the reverse charge movement at alkaline pH, $Arg^{82}$ also remains close to $Glu^{204}$, because this is its position in M$'$ and bR. Thus the amplitude of the reverse charge movement will be quite small at alkaline pH and drop with a pK between 8 and 9, as observed for the $u_2$ component and the sum $u_1 + u_2$ (Figs. 7 and 8). The remaining charge motion at alkaline pH should be due entirely to the proton transfer from $Asp^{85}$ to the Schiff base. Moreover, at alkaline pH with $Glu^{204}$ de-

protonated throughout the cycle, only one component should remain in the charge movement, as observed. The optical amplitudes are insensitive to this alkaline transition (Fig. 7 A), because the reprotonation of the Schiff base is unaffected.

3. It is well known that for closed systems (reconstituted liposomes or cells) the millisecond decay of the M intermediate is slowed down by the membrane potential, whereas its rise-time kinetics is unaffected (Quintanilha, 1980; Dancsházy et al., 1983). An exponential dependence of the rate constants on the electrical potential is expected for a barrier model. The strong voltage dependence of the steady-state photocurrent (Braun et al., 1988; Muneyuki et al., 1996) was attributed to the millisecond step in the charge translocation, which is rate limiting and involves the largest charge displacement (Braun et al., 1988; Heyn et al., 1988). Under the saturating light intensities used in our experiments, a large electric potential is built up by the first flash. The millisecond kinetics of the charge motion induced in the remaining unphotolyzed population by the second flash is therefore slowed down. This interesting phenomenon of the effect of an electric potential on the charge transfer kinetics has also been discussed elsewhere (Kleinschmidt and Hess, 1990; Nieto-Frausto et al., 1992) and explains the following two experimental observations. The amplitude of the millisecond electrical component induced by the second flash is quite small (Fig. 4), because the membrane potential generated by the first flash makes it as slow as the system discharge time. The amplitudes of the electrical back-reaction decay as a function of the delay time, with a time constant that is much longer than the normal decay of M (Fig. 6). Corresponding effects are not observed in the optical data, because those measurements were performed in gels or suspension. In the electrical measurements, on the other hand, a discharge of the potential around the edges of the membrane is prevented by the tight seal between the adsorbed membrane and the support.

## REFERENCES

Alexiev, U., R. Mollaaghababa, P. Scherrer, H. G. Khorana, and M. P. Heyn. 1995. Rapid long-range proton diffusion along the surface of the purple membrane and delayed proton transfer into the bulk. *Proc. Natl. Acad. Sci. USA.* 92:372–376.

Balashov, S. P. 1995. Photoreactions of the photointermediates of bacteriorhodopsin. *Isr. J. Chem.* 35:415–428.

Balashov, S. P., R. Govindjee, E. S. Imasheva, S. Misra, T. G. Ebrey, Y. Feng, R. K. Crouch, and D. R. Menick. 1995. The two pK$_a$'s of aspartate-85 and control of thermal isomerization and proton release in arginine-82 to lysine mutant of bacteriorhodopsin. *Biochemistry.* 34:8820–8834.

Balashov, S. P., R. Govindjee, M. Kono, E. S. Imasheva, E. Lukashev, T. G. Ebrey, R. K. Crouch, D. R. Menick, and Y. Feng. 1993. Effect of arginine-82 to alanine mutation in bacteriorhodopsin on dark adaptation,

proton release, and the photochemical cycle. *Biochemistry.* 32:10331–10343.

Balashov, S. P., E. S. Imasheva, R. Govindjee, and T. G. Ebrey. 1996. Titration of aspartate-85 in bacteriorhodopsin: what it says about chromophore isomerization and proton release. *Biophys. J.* 70:473–481.

Braiman, M. S., A. K. Dioumaev, and J. R. Lewis. 1996. A large photolysis-induced pK$_a$ increase of the chromophore counterion in bacteriorhodopsin: implication for ion transport mechanism of retinal proteins. *Biophys. J.* 70:939–947.

Braun, D., N. A. Dencher, A. Fahr, M. Lindau, and M. P. Heyn. 1988. Nonlinear voltage dependence of the light-driven proton pump current of bacteriorhodopsin. *Biophys. J.* 53:617–621.

Brown, L. S., J. Sasaki, H. Kandori, A. Maeda, R. Needleman, and J. K. Lanyi. 1995. Glutamic acid 204 is the terminal proton release group at the extracellular surface of bacteriorhodopsin. *J. Biol. Chem.* 270:27122–27126.

Dancsházy, Zs., L. A. Drachev, P. Ormos, K. Nagy, and V. P. Skulachev. 1978. Kinetics of blue light-induced inhibition of photoelectric activity of bacteriorhodopsin. *FEBS Lett.* 96:59–63.

Dancsházy, Zs., S. L. Helgerson, and W. Stoeckenius. 1983. Coupling between the bacteriorhodospin photocycle kinetics and the protonmotive force. I. Single flash measurements in *Halobacterium halobium* cells. *Photobiochem. Photobiophys.* 5:347–357.

Dancsházy, Zs., and Zs. Tokaji. 1993. Actinic light density dependence of the bacteriorhodopsin photocycle. *Biophys. J.* 65:823–831.

Dickopf, S., U. Alexiev, M. P. Krebs, H. Otto, R. Mollaaghababa, H. G. Khorana, and M. P. Heyn. 1995. Proton transport by a bacteriorhodopsin mutant, aspartic acid-85→asparagine, initiated in the unprotonated Schiff base state. *Proc. Natl. Acad. Sci. USA.* 92:11519–11523.

Druckmann, S., N. Friedman, J. K. Lanyi, R. Needleman, M. Ottolenghi, and M. Sheves. 1992. The back photoreaction of the M intermediate in the photocycle of bacteriorhodopsin: mechanism and evidence for two M species. *Photochem. Photobiol.* 56:1041–1047.

Ebrey, T. G. 1993. Light energy transduction in bacteriorhodopsin. *In* Thermodynamics of Membrane Receptors and Channels. M. B. Jackson, editor. CRC Press, Boca Raton, FL. 354–387.

Friedman, N., Y. Gat, M. Sheves, and M. Ottolenghi. 1994. On the heterogeneity of the M population in the photocycle of bacteriorhodopsin. *Biochemistry.* 33:14758–14767.

Govindjee, R., S. Misra, S. P. Balashov, T. G. Ebrey, R. K. Crouch, and D. R. Menick. 1996. Arginine-82 regulates the pK$_a$ of the group responsible for the light-driven proton release in bacteriorhodopsin. *Biophys. J.* 71:1011–1023.

Grieger, I., and G. Atkinson. 1985. Photolytic interruptions of the bacteriorhodopsin photocycle examined by time-resolved resonance Raman spectroscopy. *Biochemistry.* 24:5660–5665.

Heyn, M. P., D. Braun, N. A. Dencher, A. Fahr, M. Holz, M. Lindau, F. Seiff, I. Wallat, and J. Westerhausen. 1988. Chromophore location and charge displacement in bacteriorhodopsin. *Ber. Bunsenges. Phys. Chem.* 92:1045–1050.

Holz, M., M. Lindau, and M. P. Heyn. 1988. Distributed kinetics of the charge movements in bacteriorhodopsin: evidence for conformational substates. *Biophys. J.* 53:623–633.

Hwang, S. B., J. I. Korenbrot, and W. Stoeckenius. 1978. Transient photovoltages in purple membrane multilayers. Charge displacement in bacteriorhodopsin and its photointermediates. *Biochim. Biophys. Acta.* 509:300–317.

Kalisky, O., U. Lachish, and M. Ottolenghi. 1978. Time resolution of a back photoreaction in bacteriorhodopsin. *Photochem. Photobiol.* 28:261–263.

Kalisky, O., M. Ottolenghi, B. Honig, and R. Korenstein. 1981. Environmental effects on formation and photoreaction of the M$_{412}$ photoproduct of bacteriorhodopsin: implications for the mechanism of proton pumping. *Biochemistry.* 20:649–655.

Karvaly, B., and Zs. Dancsházy. 1977. Bacteriorhodopsin: a molecular photoelectric regulator. Quenching of photovoltaic effect of bimolecular lipid membranes containing bacteriorhodopsin by blue light. *FEBS Lett.* 76:36–40.

Kleinschmidt, C., and B. Hess. 1990. Influence of an electrical potential on the charge transfer kinetics of bacteriorhodopsin. *Biophys. J.* 58:653–663.

Kono, M., S. Misra, and T. G. Ebrey. 1993. pH dependence of light-induced proton release by bacteriorhodopsin. *FEBS Lett.* 331:31–34.

Lanyi, J. K. 1993. Proton translocation mechanism and energetics in the light-driven pump bacteriorhodopsin. *Biochim. Biophys. Acta.* 1183: 241–261.

le Coutre, J., and K. Gerwert. 1996. Kinetic isotope effects reveal an ice-like and a liquid-phase-type intramolecular proton transfer in bacteriorhodopsin. *FEBS Lett.* 398:333–336.

Liu, S. Y. 1990. Light induced currents from oriented purple membrane. I. Correlation of the microsecond component (B2) with the L-M phototransition. *Biophys. J.* 57:943–950.

Moltke, S., U. Alexiev, and M. P. Heyn. 1995. Kinetics of light-induced intramolecular charge transfer and proton release in bacteriorhodopsin. *Isr. J. Chem.* 35:401–414.

Muneyuki, E., M. Ikematsu, and M. Yoshida. 1996. $\Delta\mu H^+$ dependency of proton translocation by bacteriorhodopsin and a stochastic energization-relaxation channel model. *J. Phys. Chem.* 100:19687–19691.

Nieto-Frausto, J., P. Läuger, and H.-J. Apell. 1992. Electrostatic coupling of ion pumps. *Biophys. J.* 61:83–95.

Ohno, K., R. Govindjee, and T. G. Ebrey. 1983. Blue light effect on proton pumping by bacteriorhodopsin. *Biophys. J.* 43:251–254.

Olejnik, J., B. Brzezinski, and G. Zundel. 1992. A proton pathway with large polarizability and proton pumping mechanism in bacteriorhodopsin-Fourier transform differnce spectra of photoproducts of bacteriorhodopsin and of its pentademethyl analogue. *J. Mol. Struct.* 271:157–173.

Ormos, P., Zs. Dancsházy, and B. Karvaly. 1978. Mechanism of generation and regulation of photopotential by bacteriorhodopsin in bimolecular lipid membrane. The quenching effect of blue light. *Biochim. Biophys. Acta.* 503:304–315.

Ormos, P., Zs. Dancsházy, and L. Keszthelyi. 1980. Electric response of a back photoreaction in the bacteriorhodopsin photocycle. *Biophys. J.* 31:207–214.

Otto, H., T. Marti, M. Holz, T. Mogi, M. Lindau, H. G. Khorana, and M. P. Heyn. 1989. Aspartic acid-96 is the internal proton donor in the reprotonation of the Schiff base of bacteriorhodopsin. *Proc. Natl. Acad. Sci. USA.* 86:9228–9232.

Otto, H., T. Marti, M. Holz, T. Mogi, L. J. Stern, F. Engel, H. G. Khorana, and M. P. Heyn. 1990. Substitution of amino acids asp-85, asp-212, and arg-82 in bacteriorhodopsin affects the proton release phase of the pump and the pK of the Schiff base. *Proc. Natl. Acad. Sci. USA.* 87: 1018–1022.

Otto, H., C. Zscherp, B. Borucki, and M. P. Heyn. 1995. Time-resolved polarized absorption spectroscopy with isotropically excited oriented purple membranes: the orientation of the electronic transition dipole moment of the chromophore in the O-intermediate of bacteriorhodopsin. *J. Phys. Chem.* 99:3847–3853.

Quintanilha, A. T. 1980. Control of the photocycle in bacteriorhodopsin by electrochemical gradients. *FEBS Lett.* 117:8–12.

Richter, H.-T., L. S. Brown, R. Needleman, and J. K. Lanyi. 1996. A linkage of the $pK_a$'s of asp-85 and glu-204 forms part of the reprotonation switch of bacteriorhodopsin. *Biochemistry.* 35:4054–4062.

Sampogna, R. V., and B. Honig. 1996. Electrostatic coupling between retinal isomerization and the ionization state of Glu-204: a general mechanism for proton release in bacteriorhodopsin. *Biophys. J.* 71: 1165–1171.

Scharnagl, C., and S. F. Fischer. 1996. Conformational flexibility of arginine-82 as source for the heterogeneous and pH-dependent kinetics of the primary proton transfer step in the bacteriorhodopsin photocycle: an electrostatic model. *Chem. Phys.* 212:231–246.

Stockburger, M., W. Klusmann, H. Gattermann, G. Massig, and R. Peters. 1979. Photochemical cycle of bacteriorhodopsin studied by resonance Raman spectroscopy. *Biochemistry.* 18:4886–4900.

Takei, H., Y. Gat, M. Sheves, and A. Lewis. 1992. Low temperature FTIR study of the Schiff base reprotonation during the M to bR backphotoreaction. Asp. 85 reprotonates two distinct types of Schiff base species at different temperatures. *Biophys. J.* 63:1643–1653.

Trissl, H. W. 1990. Photoelectric measurements of purple membranes. *Photochem. Photobiol.* 51:793–818.

Zimányi, L., G. Váró, M. Chang, B. Ni, R. Needleman, and J. K. Lanyi. 1992. Pathways of proton release in the bacteriorhodopsin photocycle. *Biochemistry.* 31:8535–8543.